Desalination and Water Treatment
www.deswater.com

doi: 10.5004/dwt.2018.21837

(2018) 300–311

Removal of Reactive Black 5 and its degradation using combined treatment of nano-zerovalent iron activated persulfate and adsorption processes

T. Satapanajaru[a,b,*], C. Chokejaroenrat[a], P. Pengthamkeerati[a,b]

[a]*Department of Environmental Technology and Management, Faculty of Environment, Kasetsart University, Bangkok, Thailand, email: fscitus@ku.ac.th (T. Satapanajaru)*
[b]*Environmental Technology Special Research Unit, Faculty of Environment, Kasetsart University, Bangkok, Thailand*

Received 2 March 2017; Accepted 22 December 2017

ABSTRACT

Nano-zerovalent iron (NZVI) is best known to remediate contaminated water as a reducing agent and to activate persulfate (PS) to generate sulfate radicals for in situ and ex situ chemical oxidation technology. The objective of this study was to investigate the role of NZVI in degradation effectiveness of Reactive Black 5 (RB5) by PS in water. The removal efficiencies were determined using 400 mmol-PS/L, 4 mmol-NZVI/L, and 400 mmol-PS/L activated by 4 mmol-NZVI/L to treat 0.01 mmol-RB5/L. The highest observed removal rate constant (k_{obs}) values for RB5 and total organic carbon (TOC) removal were 3.65×10^{-2} and 1.36×10^{-2}/min, respectively, in the treatment of PS activated with NZVI. Incomplete mineralization of RB5 was observed. The removal efficiency of TOC at 120 min was only 60% ± 2% whereas that of the RB5 achieved 100%. When we increased the PS concentration and NZVI dosage, the k_{obs} value of the RB5 decolorization increased. Lowering the pH from 9 to 3 increased the degradation rates of destruction of RB5. Although the NZVI-activated PS was effective for RB5 decolorization, we found that the RB5 daughter products could be more toxic to water fleas (*Moina macrocopa*) than the original dye. Combining adsorption (fly ashes, activated carbon or any adsorbent) to the PS/NZVI-treated water provided proof-of-concept that it was safer than PS/NZVI oxidation alone in treating dye-contaminated water.

Keywords: Adsorption; Reactive Black 5; *Moina macrocopa*; Nano-zerovalent iron; Persulfate oxidation; Toxicity

1. Introduction

Effluents discharged from textile dyeing industries to public water reservoirs contain large amounts of several reactive dyes which can pose a threat to the environment and human health. Vijayaraghavan et al. [1] and Permpornsakul et al. [2] revealed that around 20%–50% of the dyes can be lost during the dyeing process, resulting in the wastewater containing around 100–200 mg/L. These dyes affect the photosynthetic activity of aquatic plants by reducing light penetration, and they may be toxic to some aquatic organisms [3]. The chemical structures of most dyestuffs are complex structured polymers with low environmental biodegradability [4]. Reactive Black 5 (RB5) is commonly found at higher concentrations than other reactive dyes in dyebath effluents [5]. RB5 contains two azo groups (–N=N–) as the chromophore, which is the basic functional group for visible color in dyes. RB5 is a well-known non-biodegradable diazo dye [6] and is popularly used in textile dyeing mills in Thailand. Moreover, RB5 was chosen as a representative of organic pollutant by several researchers [7].

Although several dye removal technologies are available such as physical, chemical, and biological methods for dye removal including: chemical coagulation, flocculation, photochemical treatment, electrochemical degradation, membrane filtration, aerobic/anaerobic biological degradation, and chemical oxidation and reduction, none of them is able to completely remove dyes from wastewater [8]. The use of living organisms in the decolorization of RB5 such as

* Corresponding author.

biosorption, microbial degradation, and bioaccumulation, may not be an option for the continuous treatment of highly concentrated effluent [1].

Nano-zerovalent iron (NZVI) technology represents one of the first generations of nanoscale usage in wastewater treatment technology. Because of its tiny size, its large specific surface area, and its high surface reactivity, NZVI has high potential in donating electrons as shown in Eq. (1):

$$\text{Nano-Fe}^0_{(s)} \rightarrow Fe^{2+} + 2e^- \quad (1)$$

This can enhance the kinetic rate of destruction of many dyes, especially, RB5. Although the color of RB5 in wastewater disappeared rapidly following NZVI treatment, RB5 was not mineralized completely. Satapanajaru et al. [9] indicated that the decolorization of RB5 by NZVI proceeded via the reductive cleavage of azo bonds resulting in the formation of amines. The 1-sulfonic,2-(4-aminobenzenesulfonyl)ethanol, with an *m*/*z* ratio of 280, resulting from N=N cleavage in the molecular structure, was one of the degradation products of RB5 by NZVI. Some researchers suggested that RB5 and its intermediates are biotoxic [10,11]. Therefore, it is necessary to transform RB5 and its intermediate into smaller molecules.

The persulfate anion ($S_2O_8^{2-}$) is a strong oxidant that is a solid at ambient temperature, thereby providing ease of storage and transport, high stability, high aqueous solubility, and relatively low cost [12,13]. However, the persulfate (PS) anion could be impeded by its slow oxidative kinetics for some contaminants. Activated PS was introduced as a robust technology to generate the sulfate radical ($SO_4^{-\bullet}$) with a standard electrode potential (E^0) of +2.60 V [14], which is only secondary to •OH radicals with an E^0 value of +2.72 V [15]. These radicals can be employed from Fenton's oxidation, ozone, and PS and can effectively destroy a broad range of organic pollutants and non-selective contaminants in wastewater [16–19]. Common PS activators include UV, transition metals, heat, and alkaline condition in accordance with the half-cell reaction Eq. (2):

$$SO_4^{-\bullet} + e^- \rightarrow SO_4^{2-}; \quad E^0 = 2.60 \text{ V} \quad (2)$$

PS oxidant has been used to treat wastewater containing dyes such as Methylene Blue [20], Acid Orange 7 [16,21], Cibacron Brilliant Yellow 3 [22], Sunset Yellow and Ponceau 4R [23], Reactive Red 45 [24], Methyl Orange [25], and RB5 [9,26]. Previous research has shown that hydrogen peroxide/UV light [27], combined sonolysis and ozonation [28], or Fenton/UV [19] were the most powerful methods to degrade RB5. The removal efficiencies of these methods were higher than 80% within a short period of time.

In this study, we quantified the degradation effectiveness of RB5 in synthetic wastewater using PS oxidation activated with NZVI. The effects of PS concentrations, NZVI dosages, initial pH levels, and particle sizes were investigated. We also conducted toxicity tests of treated water on *Moina macrocopa*, which is common in freshwater ecosystem in Thailand. *M. macrocopa* plays a key role in freshwater ecosystems and is regarded as primary consumer and a food source for other omnivorous and carnivorous animals in the higher trophic levels.

2. Materials and methods

2.1. Chemicals

RB5 Tetrasodium(6*Z*)-4-amino-5-oxo-3-[[4-(2-sulfonatooxyethylsulfonyl)phenyl]diazenyl]-6-[[4-(2-sulfonatooxyethylsulfonyl)phenyl]hydrazinylidene] naphthalene-2,7-disulfonate, as it is known under IUPAC name or Drimaren Black K-3B, Remazol Black B, C.I. Reactive Black, etc. as they are known commercially. The chemical structure of RB5 is shown in Fig. 1. RB5 (Alta Scientific Co., Ltd., China) containing 99% dye content was used in this study. Zerovalent iron (ZVI) powder was obtained from Laboratory Rasayan (India). Sodium PS (NaS_2O_8; Panreac, Barcelona, Spain), ferric chloride ($FeCl_3{\cdot}6H_2O$; Ajax Finechem, Auckland, New Zealand), sodium borohydride ($NaBH_4$; Asia Pacific Specialty Chemicals Limited, Australia), hydrochloric acid (HCl; J.T. Baker, USA), sodium hydroxide (NaOH; Carlo Erba Reagents, Italy), methanol (CH_3OH; Merck, Germany), and calcium chloride ($CaCO_3$; Ajax Finechem) were used as purchased. Activated carbon (AC) was purchased from Sigma-Aldrich (St. Louis, MO) and used as received. Adsorption of PS-treated RB5 water was tested with two types of fly ash, that is, biomass fly ash (BFA) and coal fly ash (CFA). The BFA (provided from a power station in eastern Thailand) had been oven-dried at 70°C for 24 h prior to use. The CFA was obtained from the Mae-Moh power plant located in northern Thailand and had been oven-dried at 105°C for 24 h prior to use. The physical and chemical characteristics of BFA and CFA are given in Pengthamkeerati et al. [29].

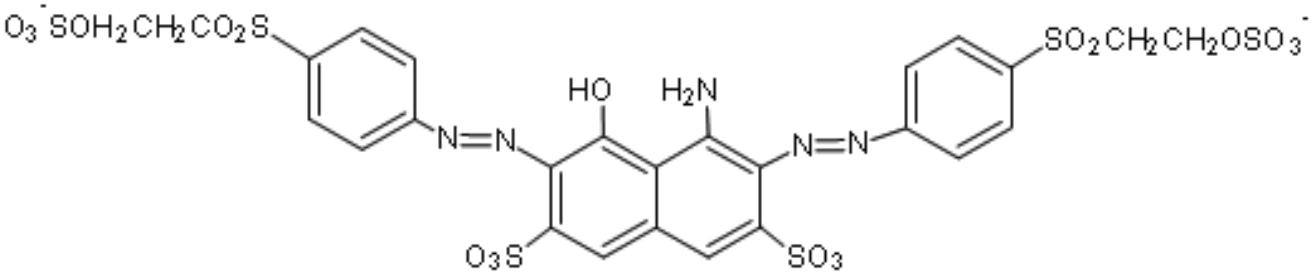

Fig. 1. Chemical structure of RB5.

2.2. Preparation of nano-zerovalent iron

To prepare nanoscale ZVI, $NaBH_4$ (0.25 mol/L) was reacted with $FeCl_3 \cdot 6H_2O$ (0.045 mol/L) in a volume ratio of 1:1 at room temperature [9]. When mixed, the ferric iron was reduced to ZVI in accordance with Eq. (3):

$$4Fe^{3+} + 3BH_4^- + 9H_2O \rightarrow 4Fe^0 + 3H_2BO_3^- + 12H^+ + 6H_2 \quad (3)$$

To avoid immediate rusting as result of NZVI oxidation, we transferred the NZVI slurry into a separate bowl, washed it with a 1:1 mixture of water and methanol, and quickly rinsed with methanol. Magnetic separation was applied in this process to partition NZVI from the slurry. Then, the NZVIs were placed in a cylindrical receptacle and blown by N_2 gas until dry.

To ensure NZVI size and uniformity, we characterized the NZVI for: the specific surface area using Quantachrome:Autosorb-1 to perform the Brunauer–Emmett–Teller (BET) method, the size and shape using a transmission electron microscope (TEM; FEI: TECNAI G2 20S-TWIN) and a scanning electron microscope (SEM; JEOL: JSM-7800F), the material structure using an X-ray diffractometer (XRD; Phillips X'Pert), and the NZVI particle size distribution using a Laser Scattering Particle Size Distribution Analyzer LA-950.

2.3. Chemical analyses

The RB5 concentration was quantified using a UV/VIS 918 spectrophotometer (Cary 60 UV-Vis Agilent Technologies) at a wavelength of 598 nm. The residual total organic carbon (TOC) was analyzed using a TOC analyzer (Tekmar Dohmann Phoenix 8000). RB5 intermediate and by-products were separated using a Zorbax SB-C18 (2.1 × 150 mm) column at a wavelength of 254 nm using the LC-MS 1200 infinity series (6490 Triple Quadrupole LC-MS Systems). We used a flow rate of 0.2 mL/min with an injection volume of 5 μL. The mobile phase was a gradient of 5:95 (MeOH:H_2O mixed with 0.05% formic acid; 10 min), 10:90 (5 min), and 100:0 (~30 min). We confirmed the degradation of the mass of RB5 using mass spectra obtained from an ion trap mass spectrometer fitted with an electron spray interface (3.5 kV) operated in positive ionization mode at a capillary temperature of 200°C.

2.4. Preliminary experimental setup

Reactivity experiments were conducted to examine the efficiency of NZVI, PS, and NZVI-activated PS. We prepare a 0.1 mmol/L RB5 stock solution and used this throughout the study. A 250 mL Erlenmeyer flask containing 100 mL DI water was spiked with an RB5 stock solution to yield the initial RB5 concentration of 0.01 mmol/L. We then treated the aqueous RB5 with a ratio of PS and NZVI (400 mmol/L:4 mmol/L (0.224 g/L), 400 mmol/L:0, or 0:4 mmol/L, respectively). The flasks were sealed with parafilm to avoid loss from evaporation. The reactors were shaken using an orbital shaker at 150 rpm at room temperature (~30°C). All experiments were run in triplicate (n = 3). Samples were selected at predetermined periodic times within 120 min. The supernatants were centrifuged at 13,000 rpm for 5 min. The residual concentrations of RB5 were quantified using UV/VIS 918 Spectrophotometer at λ = 598. TOC was analyzed using TOC analyzer (Tekmar Dohmann Phoenix 8000).

To further investigate whether RB5-treated NZVI daughter products would be prone to better degradation, we mixed 100 mL of 0.01 mmol/L RB5 with 4 mmol/L NZVI for 30 min prior to adding 400 mmol/L PS. Temporal changes in RB5 concentration and TOC were measured and analyzed as discussed earlier.

2.5. Effect of PS concentrations, NZVI dosages and pH levels on degradation of RB5 using PS oxidation activated with NZVI

To evaluate the effect of reactant concentrations and pH on RB5 degradation, we treated aqueous RB5 with at least three different values of these factors while other remains uncontrolled. For example, three concentrations of PS (200, 400, and 600 mmol/L) activated with 4 mmol/L NZVI were tested individually. In a separate experiment, we varied dosages of NZVI (2, 4, and 6 mmol/L) while we used a PS concentration of 400 mmol/L. For the pH experiment, we fixed the solution pH at 3, 5, 7, and 9 by using a specifically designed pH-stat apparatus (Metrohm Titrino 718S; Brinkman Instruments, Westbury, NY, USA), and used 0.1 mol/L HNO_3 and 0.2 mol/L NaOH to adjust the solution pH (Fig. 2). We selected 0.01 mmol/L of RB5 as the initial concentration, and 400 mmol/L PS activated with 4 mmol/L NZVI in this study. Changes in the RB5 concentrations were monitored at preselected times. The experiments were performed in triplicate and conducted at room temperature.

2.6. Effect of particle size of zerovalent iron

To study the effects of the particles size of the ZVI on degradation of RB5 by PS, three different sizes of ZVI were used, 100 mesh (≈150 μm), 325 mesh (≈44 μm), and synthesized nanosize (<100 nm). Temporal changes in the RB5 concentration were monitored by following the treatment of 400 mmol/L of PS activated with 4 mmol/L of ZVI with the different size. Experimental protocols as stated earlier were followed. Changes in the RB5 concentrations were monitored

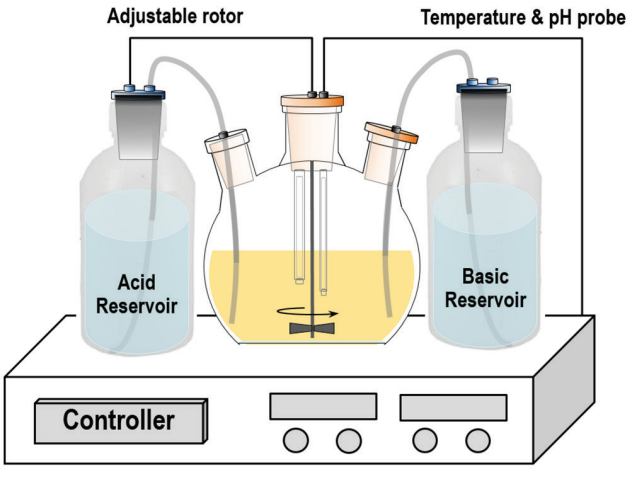

Fig. 2. Schematic diagram of pH-stat apparatus.

at preselected times. The experiment was performed in triplicate and conducted at room temperature.

2.7. Toxicity test on zooplankton

M. macrocopa was chosen in this study because it is common in freshwater ecosystems in Thailand. *M. macrocopa* was raised in 100 test tubes (16 × 150 mL) at room temperature (~30°C). *M. macrocopa* (neonate stage) aged less than 24 h from the second generation were used in the experiment. The toxicity test was based on the Organization for Economic Co-operation and Development: *Daphnia* sp., Acute Immobilisation Test 202 [30]. Toxicity tests of *M. macrocopa* were conducted in two types of experiments that differed in the successive adsorption treatment. The first set was tested in the presence of NZVI, PS, and PS/NZVI-treated RB5 water. These treated water types were subjected to a toxicity test. All solutions were diluted with DI water (50% v/v) and once again treated with 10% (w/v) of chemicals generally used in wastewater treatment practice. We selected $CaCO_3$ and AC as the main chemicals. Additionally, by-product waste from a power station in the form of fly ash was also chosen as an adsorbent, that is, BFA and CFA. Here, PS was only activated using NZVI and the RB5 initial concentration was selected at 0.01 mmol/L for all toxicity test experiments unless stated otherwise. In these tests, we observed any *M. macrocopa* movement and abnormal behavior at 24 and 48 h of exposure to these test solutions. Five replicates were run for all experiments. During each experiment, we also measured the dissolved oxygen (DO) and pH for both before and after mortality count. Calculation of LC_{50} at 24 h was performed by plotting data on the mortality of *M. macrocopa* against concentrations of RB5 for each concentration (unit: mg/L) using Probit analysis from a Probit table (Finney's table) [31].

3. Results and discussion

3.1. NZVI characterization

The SEM and TEM images showed the morphology of the NZVI particles was rough, with an aggregated, round shape, chain-like, and less than 100 nm in diameter (Figs. 3(A) and (B)). Previous research indicated that a chain-like structure with floc aggregates could be observed in laboratory made iron particles [32–34]. The NZVI particle size fraction distribution was: particle size >100 nm (9%), 100–50 nm (78%) and <50 nm (13%). The XRD result revealed

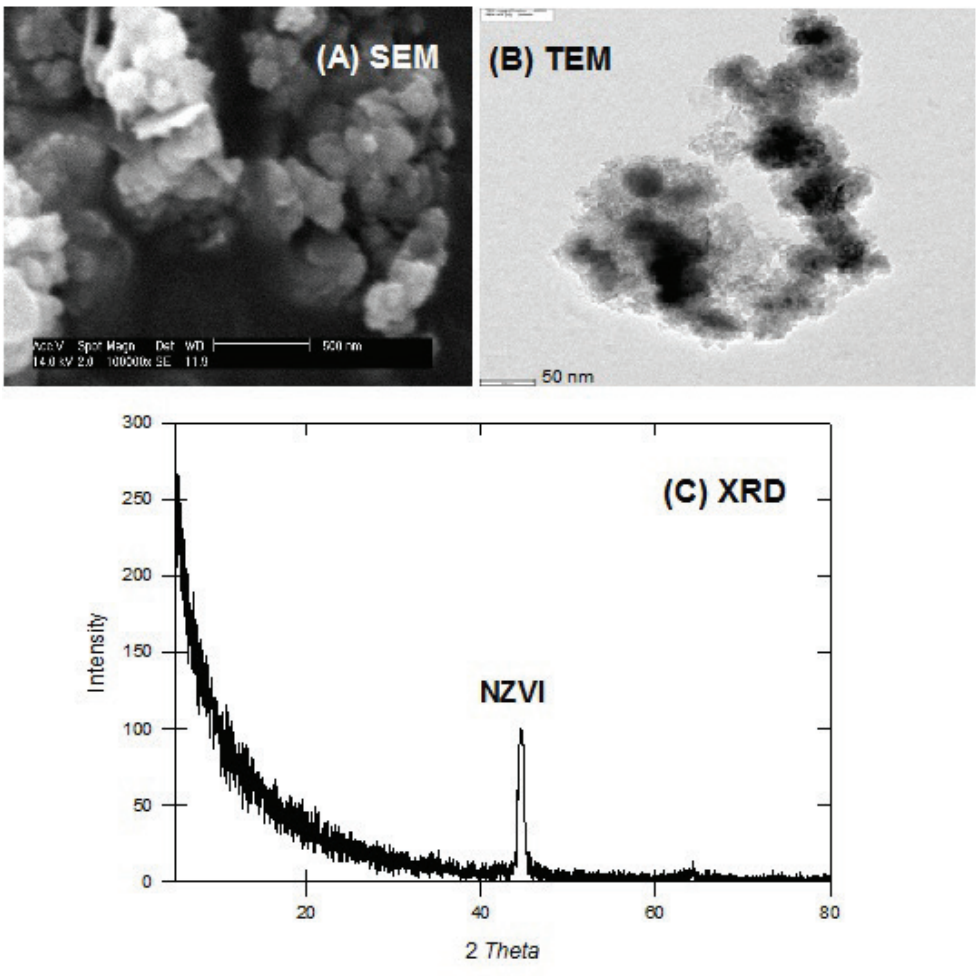

Fig. 3. NZVI particle characteristics: (A) SEM, (B) TEM and (C) XRD.

an apparent peak (44.8) at 2θ, indicating the presence of the ZVI (Fe^0; Fig. 3(C)).

Generally, Fe is mainly in its Fe^0 state by the basic reflection appearing at a 2θ value of 44.8–44.7 [34]. The BET surface area analysis indicated that the NZVI surface area was 25.65 m^2/g whereas the surface area of commercial ZVI (particle size ≈ 100 mesh) was 2.11 m^2/g. The specific surface area depends on the particle size: the more aggregated particles there are, the lower the specific surface area. Rosická and Šembera [35] noted that NZVI particles rapidly aggregate due to the magnetic forces among the nanoparticles. The magnetic field around the NZVI particles is caused by the composition of the particles. These magnetic forces contribute to the attractive forces among NZVI particles and that leads to increased aggregation of NZVI.

3.2. RB5 degradation studies

We determined the removal efficiency of RB5 using 400 mmol/L of PS, 4 mmol/L of NZVI, and 400 mmol/L of PS activated with 4 mmol/L NZVI to treat 0.01 mmol RB5 in aqueous solutions. The initial pH of the RB5 was 6.01 ± 0.09. The mineralization of RB5 was investigated on the basis of the TOC content. The degradation of RB5 and TOC by PS, NZVI, and PS with NZVI seemed to follow a pseudo-first-order degradation (Figs. 4(A) and (B)). We observed the changes in absorbance in all treatments. Changes in the UV spectrum of RB5 treated with NZVI, PS, or PS activated by NZVI resulted in a decrease in the intensity of the dye absorption band, at λ_{max} = 598 nm.

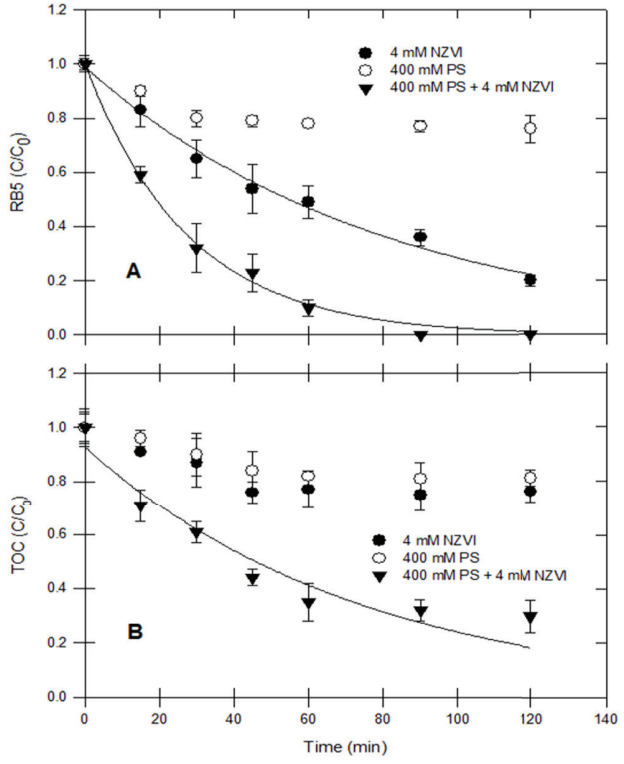

Fig. 4. Degradation of RB5 (A) and TOC (B) using 4 mM NZVI, 400 mM PS and 400 mM PS activated with 4 mM NZVI.

The observation removal rate (k_{obs}) of RB5 and TOC was calculated using Eq. (4):

$$-\frac{d[\text{RB5 or TOC}]}{dt} = k_{obs}[\text{RB5 or TOC}] \quad (4)$$

where [RB5 or TOC] is the concentration of RB5 or TOC, and t is time. In the treatment with only PS, the degradation of RB5 slowed down and reached a plateau at 60 min. The k_{obs} value for RB5 was 2.01 × 10^{-3}/min while that of TOC was 1.91 × 10^{-3}/min. The removal efficiency of RB5 at 6 h was only 20% ± 3%. The same trend was found in the study by Liang et al. [36]. Without activator (Fe), the PS anion only resulted in the production of the sulfate anion (Eq. (5)) [37]. To accelerate the degradation reaction, the PS anion must be made available via chemical activation, heat, or light which then leads to the formation of sulfate radicals.

For RB5 degradation using 4 mM NZVI resulted in the RB5 color disappearing completely within 180 min, while the TOC removal efficiency was only 25% ± 6%. The k_{obs} values for RB5 and TOC using this treatment were 1.24 × 10^{-2} and 2.46 × 10^{-3}/min, respectively. The surface normalized reaction rate constant (k_{SA}) is equal to k_{obs} divided by the specific surface area concentration (ρ_a). In this study, the specific surface area of NZVI was 10.52 m^2/g, so the ρ_a was 2.35 m^2/L. The k_{SA} is 0.527 × 10^{-2} L/m^2 min. To compare the effectiveness of destruction of RB5 and other reactive dyes by the microscale zerovalent iron (MZVI), it was found that the k_{SA} values of dye in this study were higher than those for dye degradation by MZVI by about 10–20 fold [9,38]. The decolorization of RB5 by NZVI occurs via the reductive reaction, and the reductive cleavage of the azo bonds of RB5 was accompanied by NZVI oxidation [25,26,39]. The reactions could be expressed by the following Eqs. (5)–(11):

$$2Fe^0 + 2H_2O \rightarrow 2Fe^{2+} + H_2 + 2OH^- \quad (5)$$

$$Fe^0 + O_2 + 2H^+ \rightarrow Fe^{2+} + H_2O_2 \quad (6)$$

$$Fe^{2+} + H_2O \rightarrow Fe^{3+} + 2OH^- \quad (7)$$

$$Fe^{2+} + 2OH^- \rightarrow Fe(OH)_2 \quad (8)$$

$$4Fe(OH)_2 + 2H_2O + O_2 \rightarrow 4Fe(OH)_3 \quad (9)$$

$$-N{=}N- + 2H^+ + 2e^- \rightarrow \text{-NH–NH–} \quad (10)$$

$$-NH-NH- + 2H^+ + 2e^- \rightarrow -NH_2-NH_2- \quad (11)$$

In a ZVI/water system, the zeta (ζ) potential of the iron nanoparticles as a function of solution pH and the isoelectric point was at pH ≈ 8.3 [34]. The lower the pH, the higher the positive surface charge of NZVI; however, further oxidation of the NZVI may be considered to have only limited influence on the surface characteristic [34]. In this study, the pH levels were between 6.12 and 7.59, so it is possible that the RB5 molecules (negatively charged) were absorbed on the surface of NZVI and electrons were transferred from Fe^0 to the refractory RB5 molecules, leading to the azo bonds being broken. The color of RB5 is determined by the presence of

the azo bond (-N=N-); the decolorization by NZVI proceeded via the reductive cleavage of the azo bond, resulting in the formation of amines and the color disappeared.

Another option is that NZVI reacted with water molecules and generated hydrogen ions which might be able to reduce RB5 to organic amine [40]. Previous research confirmed that the loss of RB5 color was due to the reductive of N=N cleavage in the molecular structure in the dye molecules [7,9,26,39]. However, the lower reduction of TOC indicated that there were high amounts of organic molecules remaining in the NZVI/RB5/water system. These molecules might contain functional groups that are resistant to reduction in a reducing environment, for example, amine, carboxylic, aromatic rings [41]. Guo et al. [42] and Li et al. [40] indicated that substituted aromatic amine, the dominant by-product of the degradation of the dye, Methyl Orange, using zerovalent zinc, caused incomplete mineralization.

When NZVI was used to activate the PS reaction, the concentrations of both RB5 and TOC were significantly decreased. The k_{obs} values for RB5 and TOC in this treatment were 3.65×10^{-2} and 1.36×10^{-2}/min, respectively. The kinetic rate constants of the RB5 degradation were three times higher than those of the RB5 treated using NZVI alone. The removal efficiencies of RB5 and TOC at 120 min were 100% and 60% ± 2%, respectively. Kusic et al. [24] indicated that the ZVI/PS process yielded 53.36% mineralization of azo dye whereas only 34.89% mineralization was achieved using ferrous ion/PS. The stoichiometric reactions between PS and NZVI are expressed by the following Eqs. (12)–(18):

$$S_2O_8^{2-} + 2Fe^{2+} \rightarrow 2Fe^{3+} + 2SO_4^{-\bullet} \quad (12)$$

$$S_2O_8^{2-} + Fe^{2+} \rightarrow 2Fe^{3+} + SO_4^{2-} + SO_4^{-\bullet} \quad (13)$$

$$Fe^{2+} + SO_4^{-\bullet} \rightarrow Fe^{3+} + SO_4^{2-} \quad (14)$$

$$SO_4^{-\bullet} + H_2O \rightarrow SO_4^{2-} + H^+ + HO^\bullet \text{ (hydroxyl radical)} \quad (15)$$

$$SO_4^{-\bullet} + HO^\bullet + RB5 \rightarrow SO_4^{2-} + OH^- + \text{intermediates} \quad (16)$$

$$Fe^0 + RB5 \rightarrow Fe^{2+} + \text{intermediates} \quad (17)$$

$$Fe^{2+} + RB5 \rightarrow Fe^{3+} + \text{intermediates} \quad (18)$$

Because of its tiny size, its large specific surface area and its high surface reactivity, NZVI has effective electron-donating capacity and generates the ferrous ion (Fe^{2+}) rapidly. The electrons attach to an azo bond directly, whereas Fe^{2+} quickly activates the reaction of PS. Fe^{2+} is important as it can catalyze PS to produce sulfate radicals and its existence can affect the removal efficiency of organic pollutant significantly [13].

The proposed pathway of RB5 degradation is shown in Fig. 5. Possible intermediates or by-products of RB5 degradation by PS activated by NZVI were identified using LC-MS. The samples were collected during the treatment (30, 60, and 120 min). In the first step, the initial reductive cleavage of the azo bonds results in the RB5 molecule being converted into two intermediates, 1,7-sulfonic, 2,7,8-triaminonaphthalen-1-ol (Fig. 5(A)) and 4-(ethylsulfonyl)sulfonic benzoamine (Fig. 5(B)), as mentioned earlier. Then, the $NaSO_3$ groups are removed by H^+. These intermediates are shown in Fig. 5(C) for 2,7,8-triaminonaphthalen-1-ol, *m*/*z* ratio of 189 and Fig. 5(F) for 4-(ethylsulfonyl)benzoamine, with an *m*/*z* ratio of 185. With the 2,7,8-triaminonaphthalen-1-ol route, the NH_2 functional group are removed by $SO_4^{-\bullet}$ or $HO^\bullet$. Naphthol (Fig. 5(D)) is formed, with an *m*/*z* ratio of 144. Subsequently, the aromatic ring is opened by these oxidants as shown in Fig. 5(E). Then, phenol (Fig. 5(H)), with an *m*/*z* ratio of 94, is formed. The 4-(ethylsulfonyl)benzoamine route, involves the removal of the ethylsulfonyl group by these oxidants. Benzoamine (Fig. 5(G)) is attached by $HO^\bullet$ resulting in phenol. Phenol is the major intermediate in both routes. The degradation of phenol leads to organic acids, then the organic acids are finally oxidized to carbon dioxide and water. Phenol is probably oxidized to catechol and hydroquinone which are further oxidized to *o*-benzoquinone and *p*-benzoquinone, respectively [16,43]. Homlok et al. [44] concluded that the hydroxyl radical initiated oxidation of phenols; the one-electron oxidant $^\bullet OH$ when DO is present induces two–four electron oxidations. Zhang et al. [45] reported that the degradation of phenol led to *p*-benzoquinone and ring cleavage product of maleic acids. Vasconcelos et al. [7] proposed a pathway of RB5 degraded by electrochemical methods. They also found that hydroquinone and catechol are formed from phenol in the limiting steps of RB5 oxidation. The *o*-benzoquinone and *p*-benzoquinone may be decomposed to organic

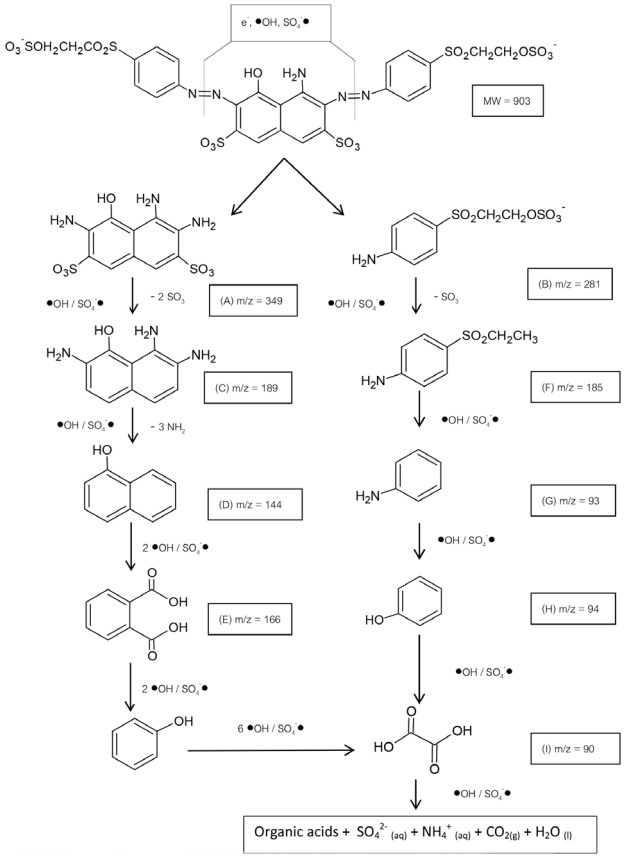

Fig. 5. Proposed pathway of RB5 degradation by PS oxidation activated by NZVI.

acids such as acetic acid, formic acid, propionic acid, and fumaric acid, which are then oxidized to carbon dioxide and water [46].

Another experiment was performed under the assumption that a smaller chemical structure would result in better degradation. The 0.01 mmol/L RB5 was treated using NZVI to break down the azo bond, then, after 30 min, PS was added into the system. After adding PS, the k_{obs} values for both RB5 and TOC increased significantly (Fig. 6). The k_{obs} values for RB5 and TOC with this treatment were 6.27×10^{-2} and 2.82×10^{-3}/min, respectively. The removal of TOC (80% ± 7%) at 120 min was higher than that of our previous treatment. The molecular size and structure have effects on the degradation of organic chemicals by PS oxidation. Homlok et al. [44] indicated that the high oxidation rates were explained by radical addition to unsaturated bonds and subsequent reactions of DO with organic radicals. In amino substituted molecules or in Acid Red 1 azo dye, O_2 was not able to compete efficiently with the unimolecular transformation of organic radicals and the efficiency was low.

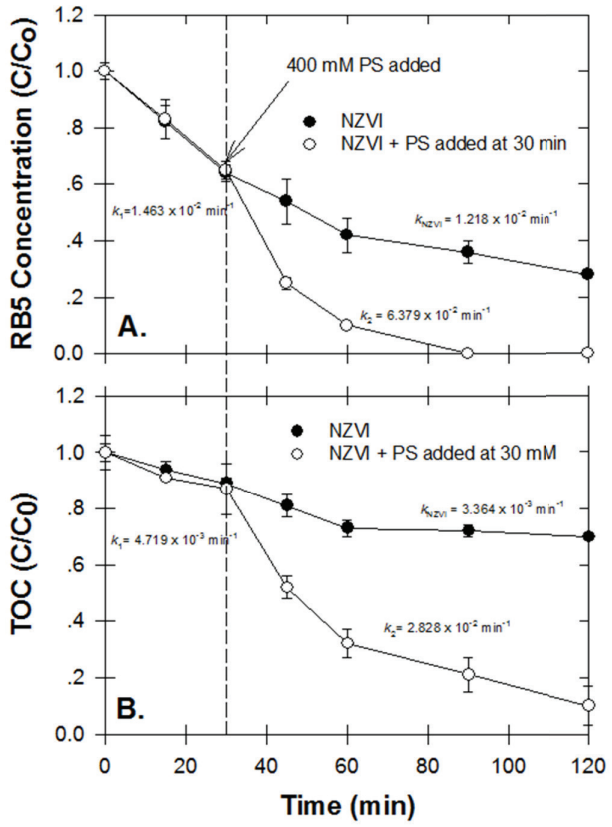

Fig. 6. Degradation of RB5 (A) and TOC (B) when 400 mM PS was added to 4 mM NZVI after 30 min of the experiment.

3.3. Effect of PS concentrations and NZVI dosages

The effects of PS concentration and NZVI dosages on the degradation of RB5 using PS oxidation were investigated. When the PS concentration increased from 200 to 600 mM with a fixed NZVI dosage, the k_{obs} values of RB5 degradation increased from 1.73×10^{-2} to 5.51×10^{-2}/min (Table 1; Fig. 7). The same trend was found when the NZVI dosages were increased from 2 to 6 mmol/L. The k_{obs} values of RB5 degradation increased from 1.38×10^{-2} to 8.06×10^{-2}/min (Table 1; Fig. 7). For the reduction of TOC (Table 1), when the PS concentration increased from 200 to 600 mM with a fixed NZVI dosage, the k_{obs} values of TOC removal increased. Moreover, when the NZVI dosages were increased from 2 to 6 mmol/L, the k_{obs} values of TOC removal also increased. The lower removal of TOC indicated that there were high amounts of organic molecules remaining in the NZVI/RB5/PS/water system. These molecules might contain functional groups that are resistant to reduction in a reducing environment, for example, amine, carboxylic, aromatic rings [40–42].

PS and NZVI, as catalysts, play an important role together to generate $SO_4^{\bullet-}$, while a further increase in the PS and NZVI concentration resulted in a higher k_{obs} as has been reported by other researchers [47,48]. However, the excessive amount of PS oxidant had a detrimental effect on the degradation efficiency [13,49]. It is possible that, when the PS concentration in the dye/PS/ZVI system is excessive, the sulfate radicals would be consumed via Eqs. (19) and (20):

$$SO_4^{\bullet-} + S_2O_8^{2-} \rightarrow 2SO_4^{-} + S_2O_8^{2-\bullet} \quad (19)$$

$$SO_4^{\bullet-} + SO_4^{\bullet-} \rightarrow S_2O_8^{2-} \quad (20)$$

However, an increase in the PS concentration from 400 to 600 nm resulted in a slight increase in RB5 degradation.

Table 1
Removal rate constants of RB5 degradation by PS activated by NZVI

Experiment	PS (mM)	NZVI (mM)	RB5		TOC	
			Removal (%)	k_{obs} (min^{-1})	Removal (%)	k_{obs} (min^{-1})
A	0	4	84	1.24×10^{-2}	24	0.25×10^{-2}
B	400	0	22	0.20×10^{-2}	17	0.19×10^{-2}
C	400	2	74	1.38×10^{-2}	55	0.92×10^{-3}
D	400	4	98	3.65×10^{-2}	72	1.36×10^{-2}
E	400	6	100	8.06×10^{-2}	80	1.45×10^{-2}
F	200	4	79	1.73×10^{-2}	45	0.84×10^{-3}
G	600	4	99	5.51×10^{-2}	86	1.52×10^{-2}

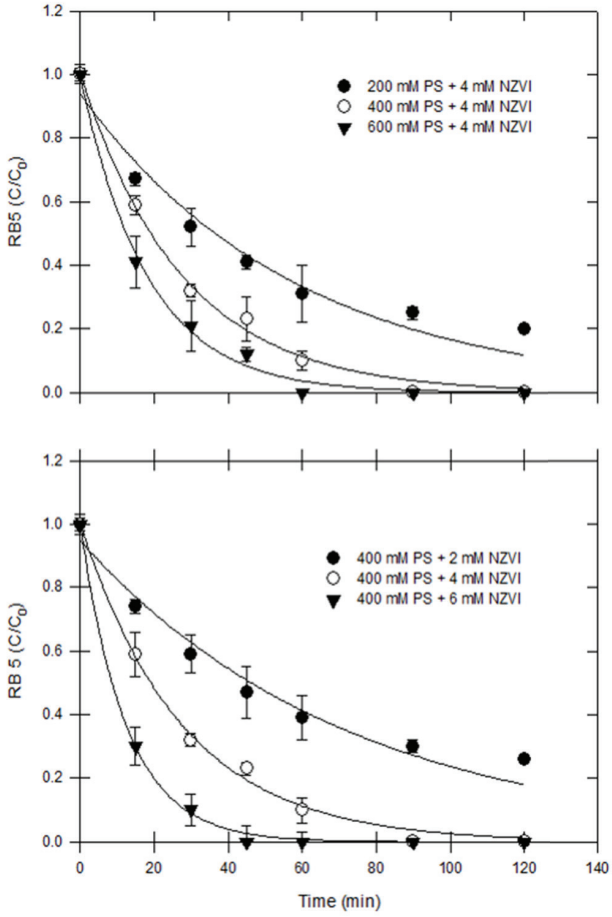

Fig. 7. Effects of PS concentration (A) and NZVI dosage (B) on degradation of RB5.

The same results were found for the degradation of azo dye using PS activated by ferrous ion [13] and ZVI [25,26,48].

The higher RB5 degradation efficiency at the higher dosage of NZVI might have resulted from the fact that NZVI generated more electrons and produced more Fe^{2+}. Electrons can attach to the azo bond directly whereas Fe^{2+} can activate PS to produce sulfate radicals. However, excessive Fe^{2+} can act as a sulfate radical scavenger. Xu and Li [13] found that the concentration of Fe^{2+} was consumed rapidly once the PS reaction was initiated and most Fe^{2+} ions were transformed to Fe^{3+} after several minutes.

3.4. Effect of initial pH

The pH value is important in the ZVI/water system because the corrosion of ZVI is influence by H^+. Lowering the initial pH improved the degradation rate of RB5. The k_{obs} values for RB5 degradation using PS activated by NZVI at pH 3, 5, 7, 9, and 11 were 4.72×10^{-2}, 3.95×10^{-2}, 3.41×10^{-2}, 1.54×10^{-2}, and 0.61×10^{-3}/min, respectively (Fig. 8).

Our results revealed that lowering the pH improved the RB5 degradation as it causes the rapid disappearance of NZVI under acidic conditions. Due to the rapid oxidation of NZVI once exposed to water and/or air, most NZVI

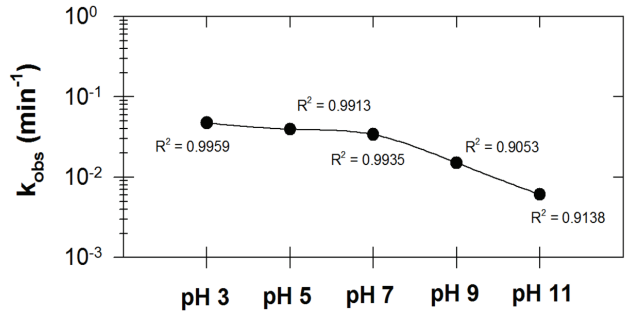

Fig. 8. k_{obs} at varying pH of RB5 degradation with 400 mM PS activated with NZVI.

completely transformed to Fe^{2+} and the Fe^{2+} reacted quickly with the PS in the system. Huang and Huang [50] studied the types of free radicals present during PS oxidation in aqueous solution using electron spin resonance at different pH levels, and found that the sulfate radical is the major free radical under acidic and neutral conditions (pH 2–7). Zhao et al. [51] and Wang et al. [48] indicated that the reaction of ZVI and PS was thermodynamically favorable; it was a slow process at a near neutral pH of 5.8 because the amount of Fe^{2+} was limited since passivation films on the ZVI surface prevented the sequential dissolution of ZVI. It is known that ZVI reacts with water in an aqueous environment to form a layer of oxyhydroxide (–OOH) on the iron surface [39]. Yan et al. [52] found that the sulfate radical was able to convert to hydroxyl radicals under alkaline conditions (Eq. (21)). The scavenging reaction between sulfate radicals and hydroxyl radicals could occur at high pH values according to Eq. (22) [48,53]:

$$SO_4^{-\bullet} + OH^- \rightarrow SO_4^{2-} + HO^\bullet \quad (21)$$

$$SO_4^{-\bullet} + HO^\bullet \rightarrow 2SO_4^- + 0.5O_2 \quad (22)$$

Previous research observed similar results for the PS oxidation process of dye at different pH levels [9,13,40,47].

3.5. Effect of particle size

We determined the removal efficiency of RB5 using PS activated with different particle sizes of ZVI. The k_{obs} values for RB5 degradation using PS activated by 150 μm, 44 μm, and NZVI (<100 nm) were 1.74×10^{-2}, 2.33×10^{-2}, and 3.84×10^{-2}/min, respectively (Fig. 9).

Our results indicated that the NZVI size was influential in the activation of PS and the degradation of RB5. In the water/ZVI system, ZVI is a precursor of Fe^{2+}, and the smaller the particle size, the higher the yield of Fe^{2+}. NZVI (<100 nm) possesses the advantages of a larger specific surface area and higher surface activities over micro and powder iron, which can enhance the chemical reaction rate of degradable contaminants [54]. Li et al. [40] studied the influence of the particle size of ZVI on the reactivity of activated PS for Acid Orange 7. They found that ZVI types with different particle sizes and specific surface areas showed potential to activate PS to produce sulfate radicals with NZVI (50 nm) > micro-ZVI (150 μm) > milli-ZVI (1 mm).

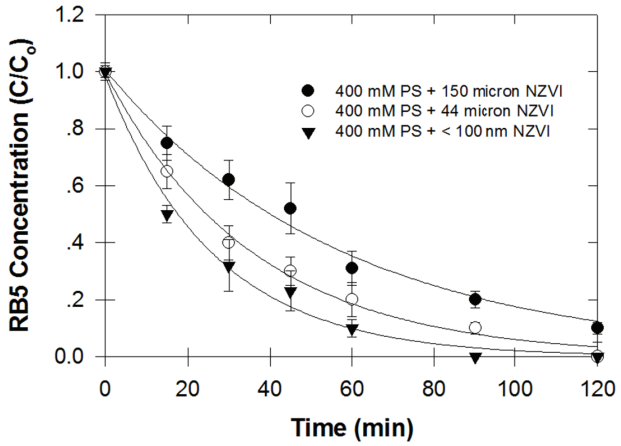

Fig. 9. RB5 degradation with 400 mM PS activated with NZVI under different particle sizes of NZVI.

3.6. Toxicity test

The results of the toxicity test of RB5 on the aquatic invertebrate, *M. macrocopa*, revealed that the LC_{50} of RB5 for *M. macrocopa* was 58.32 ± 13.24 mg/L. The material safety data sheet indicated RB5 is toxic to fish (*Leuciscus idus*, LC_{50} > 100 mg/L at 48 h). Vinitnantharat et al. [55] found the LC_{50} values of Basic Red 14 and Reactive Red 141 for *M. macrocopa* were 4.9 and 18.2 mg/L, respectively. We also tested toxicity for 0.01 nm RB5 (100 mL) and 0.01 mmol/L RB5 were treated using NZVI, PS, and PS activated by NZVI on water fleas (*M. macrocopa* – neonate stage). The pH levels for 0.0 nm RB5 and 0.01 mmol/L RB5 were treated with NZVI, PS, and PS activated by NZVI were 6.01, 7.42, 4.13, and 5.02, respectively. Photographs of water flea were taken which exposed to DI water, RB5, RB5 contaminated water treated with PS for 1 d, and RB5 contaminated water treated with PS and NZVI for 1 d and investigated for differences between the conditions (Fig. 10).

Our results indicated that black dye was presented on the external body and internal system of the water fleas. The results revealed that all treatment tests were toxic to water fleas as indicated by the high flea mortality levels. In order to test whether or not PS-treated RB5 water had an effect on zooplanktons, we conducted toxicity test experiments using various solutions of treated water. The initial results showed that *M. macrocopa* did not survive in RB5 water treated with PS, and NZVI-activated PS (percentage mortality of ~100%, Fig. 11). This was due to the instant decrease in the pH which resulted from the HO^- and H^+ generation during decolorization of RB5 by SO_4^{--} and toxic from the degradation products [56]. The same trend was reported by Chang et al. [57] who found the toxicity of CI. Acid Black 1 solution treated using Fenton oxidation was higher than that using the ZVI/air treatment. De Luna et al. [18] evaluated the ecotoxicity of five dyes to freshwater organisms before and during their photo-Fenton degradation. Their toxicity tests revealed that although the applied treatment was effective for the decolorization of the dye, partial mineralization may be responsible for the presence of degradation products which can be more toxic than the original dye, as is the case with Vat Green 3 and RB5, leading to initially toxic products.

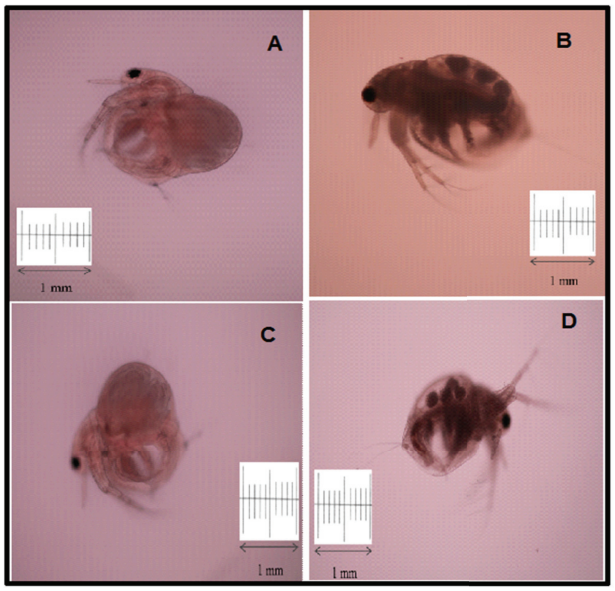

Fig. 10. Photograph of the *Moina macrocopa* exposed in different aqueous solution: (A) DI water, (B) RB5 solution, (C) persulfate-treated RB5 water, and (D) NZVI and persulfate-treated RB5 water.

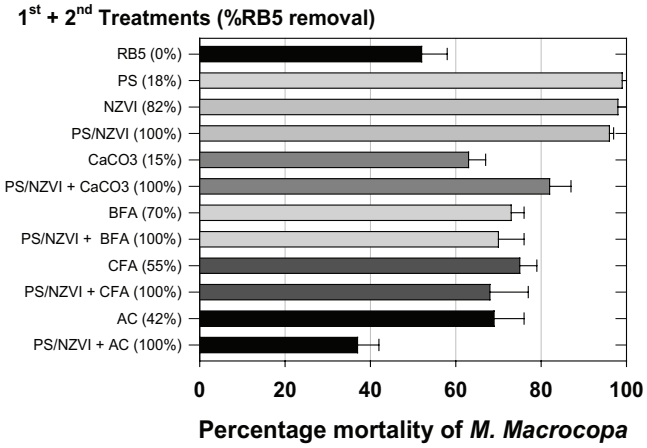

Fig. 11. Percentage mortality of *Moina macrocopa* cultured in treated water.

Because it is unlikely that PS-treated water would be disseminated directly to the receiving watershed, we treated this water with AC (10% w/v) that was subsequently diluted with DI water (50% v/v) and later conducted the toxicity tests with these water samples as described earlier.

Second adsorption treatments had lower percentage mortality rates than oxidation (PS and PS/NZVI) and reduction (NZVI) alone. We selected $CaCO_3$ as it is generally used in wastewater treatment and it can neutralize the solution pH from the production of H^+. However, the percentage mortality of *M. macrocopa* was still high (>80%). We have previously considered that RB5 derivatives may cease *M. macrocopa* [58]. We further tested if two different fly ashes would decrease the mortality percentage at the same time. Both BFA and CFA were capable of acting as an industrial adsorbent, however,

the adsorption capacity of both fly ashes was different. Pengthamkeerati et al. [29] reported that the different adsorption capacities of these two fly ashes could be attributed to different physical and chemical properties. CFA provided a much smaller specific surface area (3.39 m^2/g) whereas the specific surface area of BFA was 14.32 m^2/g. Moreover, the major chemical composition of CFA is SiO_2, Al_2O_3, and Fe_2O_3 whereas BFA contains unburned carbon which may partly contribute to the high adsorption capacity [29]. However, BFA alone was able to remove 70% RB5 while CFA removed 55% (Fig. 9). Using BFA or CFA may be beneficial as the presence of trace concentration of heavy metals in either fly ash [59] that could concomitantly activate the PS and yield $SO_4^{\bullet-}$. Although $SO_4^{\bullet-}$ oxidation was successful in decolorizing azo dye [25], complete removal of RB5 transformation products is still necessary. The mortality percentage from PS/NZVI and adsorption of both fly ashes was still high (~69%). In an attempt to remove RB5 and its transformation products from water, we tested AC in the same manner. We observed that AC not only had good adsorption of the derivatives; but it also increased the pH, thereby reducing toxicity (~37%). The particle size, surface area, and pore of AC used in this study were 12–24 mesh, 600 m^2/g, and 0.95 mL/g dry basis, respectively. Because of its small size and surface area, AC provided the best adsorption efficiency in both RB5 and degradation products. Heibati et al. [60] studied the adsorption mechanism of RB5 on walnut activated carbon (WAC). They found that the adsorption behavior and mechanism of RB5 for WAC happen via surface adsorption followed by diffusion into the pores of the WAC. As we mentioned earlier, phenol may be a major derivative of degradation of RB5 by PS. AC is one of the effective adsorbents for removal of phenol from aqueous solution. Equilibrium data fitted to the Langmuir model with a maximum phenol adsorption capacity by AC produced from biomass materials of 149.25 mg/g [61]. Therefore, the combination treatment between PS activated by NZVI and adsorption process might be a safe and effective treatment method for treating dye-contaminated water.

4. Conclusion

We determined the removal efficiency of RB5 using 400 mmol/L of PS, 4 mmol/L of NZVI, and 400 mmol/L PS activated by 4 mmol/L NZVI to treat 0.01 mmol/L RB5 in aqueous solutions. The highest k_{obs} values for RB5 and TOC removal were 3.65×10^{-2} and 1.36×10^{-2}/min in the treatment of PS activated by NZVI. However, PS activated NZVI was not able to complete the mineralization. The removal efficiency of TOC at 120 min was only 60% ± 2%. When the PS and NZVI dosages increased, the k_{obs} of the RB5 decolorization increased. In addition, lowering the pH from 9 to 3 increased the kinetic rates of destruction of RB5. The smaller the particle size, the higher the degradation kinetic rates. Although the PS activated by NZVI treatment was effective for the decolorization of the RB5, disadvantages of this method are the formation of iron oxides leading to problem of sediments and flocculation in treatment system and the toxic intermediates occurred during the reactions. The incomplete mineralization may be responsible for the presence of intermediates and by-products either of which could be more toxic than the original dye. Our results indicated that *M. macrocopa* plays a key role in freshwater ecosystems and did not survive in RB5 water treated with PS, and NZVI-activated PS (percentage mortality of ~100%). We suggest that treated water should be treated secondary before releasing to natural water resources. Combining adsorption (BFA, CFA, AC, or other adsorbents) to the PS/NZVI-treated water provided proof-of-concept that it was safer than PS/NZVI oxidation alone.

Acknowledgments

This research was supported by The Kasetsart University Research and Development Institute (KURDI) and the Department of Environmental Technology and Management, Faculty of Environment, Kasetsart University, Bangkok, Thailand. We also thank Miss Maneekarn Yoo-iam and Miss Pornphun Lertkijmankong for their research assistance.

References

[1] J. Vijayaraghavan, S.J.S. Basha, J. Jegan, A review on efficacious methods to decolorize reactive azo dye, J. Urban Environ. Eng., 7 (2013) 30–47.
[2] P. Permpornsakul, S. Prasongsuk, P. Lotrakul, D.E. Eveleigh, D.Y. Kobayashi, T. Imai, H. Punnapayak, Biological treatment of Reactive Black 5 by resupinate white rot fungus *Phanerochaete sordida* PBU 0057, Pol. J. Environ. Stud., 25 (2016) 1167–1176.
[3] H. Zollinger, Color Chemistry: Syntheses, Properties, and Applications of Organic Dyes and Pigments, 3rd revised edition, VHCA, Verlag Helvetica ChimicaActa, Zurich, 2003.
[4] U. Bali, E. Çatalkaya, F. Şengül, Photodegradation of reactive black 5, direct red 28 and direct yellow 12 using UV, UV/H_2O_2 and UV/H_2O_2/Fe^{2+}: a comparative study, J. Hazard. Mater., 114 (2004) 159–166.
[5] C.-H. Yu, C.-H. Wu, T.-H. Ho, P.K.A. Hong, Decolorization of CI Reactive Black 5 in UV/TiO_2, UV/oxidant and UV/TiO_2/oxidant systems: a comparative study, Chem. Eng. J., 158 (2010) 578–583.
[6] E. Kusvuran, S. Irmak, H.I. Yavuz, A. Samil, O. Erbatur, Comparison of the treatment methods efficiency for decolorization and mineralization of Reactive Black 5 azo dye, J. Hazard. Mater., 119 (2005) 109–116.
[7] V.M. Vasconcelos, F.L. Ribeiro, F.L. Migliorini, S.A. Alves, J.R. Steter, M.R. Baldan, N.G. Ferreira, M.R.V. Lanza, Electrochemical removal of Reactive Black 5 azo dye using non-commercial boron-doped diamond film anodes, Electrochim. Acta, 178 (2015) 484–493.
[8] N. Dizge, C. Aydiner, E. Demirbas, M. Kobya, S. Kara, Adsorption of reactive dyes from aqueous solutions by fly ash: kinetic and equilibrium studies, J. Hazard. Mater., 150 (2008) 737–746.
[9] T. Satapanajaru, C. Chompuchan, P. Suntornchot, P. Pengthamkeerati, Enhancing decolorization of Reactive Black 5 and Reactive Red 198 during nano zerovalent iron treatment, Desalination, 266 (2011) 218–230.
[10] S.-H. Chang, K.-S. Wang, H.-H. Liang, H.-Y. Chen, H.-C. Li, T.-H. Peng, Y.-C. Su, C.-Y. Chang, Treatment of Reactive Black 5 by combined electrocoagulation-granular activated carbon adsorption-microwave regeneration process, J. Hazard. Mater., 175 (2010) 850–857.
[11] K.-s. Wang, H.-Y. Chen, L.-C. Huang, Y.-C. Su, S.-H. Chang, Degradation of Reactive Black 5 using combined electrochemical degradation-solar-light/immobilized TiO_2 film process and toxicity evaluation, Chemosphere, 72 (2008) 299–305.
[12] T.K. Lau, W. Chu, N.J.D. Graham, The aqueous degradation of butylated hydroxyanisole by UV/$S_2O_8^{2-}$: study of reaction mechanisms via dimerization and mineralization, Environ. Sci. Technol., 41 (2007) 613–619.
[13] X.-R. Xu, X.-Z. Li, Degradation of azo dye Orange G in aqueous solutions by persulfate with ferrous ion, Sep. Purif. Technol., 72 (2010) 105–111.

[14] G.R. Peyton, The free-radical chemistry of persulfate-based total organic carbon analyzers, Mar. Chem., 41 (1993) 91–103.
[15] G.V. Buxton, T.N. Malone, G.A. Salmon, Reaction of $SO_4^{-\bullet}$ with Fe^{2+}, Mn^{2+} and Cu^{2+} in aqueous solution, J. Chem. Soc., Faraday Trans., 93 (1997) 2893–2897.
[16] S. Yang, P. Wang, X. Yang, L. Shan, W. Zhang, X. Shao, R. Niu, Degradation efficiencies of azo dye Acid Orange 7 by the interaction of heat, UV and anions with common oxidants: persulfate, peroxymonosulfate and hydrogen peroxide, J. Hazard. Mater., 179 (2010) 552–558.
[17] C. Sakulthaew, S. Comfort, C. Chokejaroenrat, C. Harris, X. Li, A combined chemical and biological approach to transforming and mineralizing PAHs in runoff water, Chemosphere, 117 (2014) 1–9.
[18] L.A.V. De Luna, T.H.G. da Silva, R.F.P. Nogueira, F. Kummrow, G.A. Umbuzeiro, Aquatic toxicity of dyes before and after photo-Fenton treatment, J. Hazard. Mater., 276 (2014) 332–338.
[19] M.S. Lucas, J.A. Peres, Degradation of Reactive Black 5 by Fenton/UV-C and ferrioxalate/H_2O_2/solar light processes, Dyes Pigm., 74 (2007) 622–629.
[20] P. Gayathri, R.P.J. Dorathi, K. Palanivelu, Sonochemical degradation of textile dyes in aqueous solution using sulfate radicals activated by immobilized cobalt ions, Ultrason. Sonochem., 17 (2010) 566–571.
[21] S. Yang, X. Yang, X. Shao, R. Niu, L. Wang, Activated carbon catalyzed persulfate oxidation of Azo dye acid orange 7 at ambient temperature, J. Hazard. Mater., 186 (2011) 659–666.
[22] M.C. Yeber, L. Díaz, J. Fernández, Catalytic activity of the SO_4^- radical for photodegradation of the azo dye Cibacron Brilliant Yellow 3 and 3,4-dichlorophenol: optimization by application of response surface methodology, J. Photochem. Photobiol., A, 215 (2010) 90–95.
[23] A.H. Gemeay, A.-F.M. Habib, M.A.B. El-Din, Kinetics and mechanism of the uncatalyzed and Ag(I)-catalyzed oxidative decolorization of Sunset Yellow and Ponceau 4R with peroxydisulphate, Dyes Pigm., 74 (2007) 458–463.
[24] H. Kusic, I. Peternel, N. Koprivanac, A. Loncaric Bozic, Iron-activated persulfate oxidation of an azo dye in model wastewater: influence of iron activator type on process optimization, J. Environ. Eng., 137 (2010) 454–463.
[25] C. Chokejaroenrat, C. Sakulthaew, T. Satapanajaru, T. Tikhamram, A. Pho-Ong, T. Mulseesuk, Treating methyl orange in a two-dimensional flow tank by in situ chemical oxidation using slow-release persulfate activated with zero-valent iron, Environ. Eng. Sci., 32 (2015) 1007–1015.
[26] T. Satapanajaru, M. Yoo-iam, P. Bongprom, P. Pengthamkeerati, Decolorization of Reactive Black 5 by persulfate oxidation activated by ferrous ion and its optimization, Desal. Wat. Treat., 56 (2015) 121–135.
[27] A.M. El-Dein, J.A. Libra, U. Wiesmann, Mechanism and kinetic model for the decolorization of the azo dye Reactive Black 5 by hydrogen peroxide and UV radiation, Chemosphere, 52 (2003) 1069–1077.
[28] Z. He, S. Song, H. Zhou, H. Ying, J. Chen, CI Reactive Black 5 decolorization by combined sonolysis and ozonation, Ultrason. Sonochem., 14 (2007) 298–304.
[29] P. Pengthamkeerati, T. Satapanajaru, O. Singchan, Sorption of reactive dye from aqueous solution on biomass fly ash, J. Hazard. Mater., 153 (2008) 1149–1156.
[30] Organisation for Economic and Development, Test No. 202: *Daphnia* sp. Acute Immobilisation Test, OECD Publishing, 2004.
[31] D.J. Finney, Probit analysis, 3rd Edition, Cambridge University Press, Cambridge, 1971.
[32] Y. Zhang, W. Chen, C. Dai, C. Zhou, X. Zhou, Structural evolution of nanoscale zero-valent iron (nZVI) in anoxic Co^{2+} solution: interactional performance and mechanism, Sci. Rep., 5 (2015) 53966.
[33] Ç. Üzüm, T. Shahwan, A.E. Eroğlu, I. Lieberwirth, T.B. Scott, K.R. Hallam, Application of zero-valent iron nanoparticles for the removal of aqueous Co^{2+} ions under various experimental conditions, Chem. Eng. J., 144 (2008) 213–220.
[34] Y.-P. Sun, X.-q. Li, J. Cao, W.-x. Zhang, H.P. Wang, Characterization of zero-valent iron nanoparticles, Adv. Colloid Interface Sci., 120 (2006) 47–56.
[35] D. Rosická, J. Šembera, Influence of structure of iron nanoparticles in aggregates on their magnetic properties, Nanoscale Res. Lett., 6 (2011) 527.
[36] C. Liang, I.-L. Lee, I.-Y. Hsu, C.-P. Liang, Y.L. Lin, Persulfate oxidation of trichloroethylene with and without iron activation in porous media, Chemosphere, 70 (2008) 426–435.
[37] W.M. Latimer, Oxidation Potentials, Prentice-Hall, Inc., Englewood Cliffs, NJ, 1952.
[38] C. Chompuchan, T. Satapanajaru, P. Suntornchot, P. Pengthamkeerati, Decolorization of Reactive Black 5 and Reactive Red 198 using nanoscale zerovalent iron, Proc. World Acad. Sci. Eng. Technol., 37 (2009) 130–134.
[39] S. Chatterjee, S.-R. Lim, S.H. Woo, Removal of Reactive Black 5 by zero-valent iron modified with various surfactants, Chem. Eng. J., 160 (2010) 27–32.
[40] H. Li, J. Wan, Y. Ma, Y. Wang, M. Huang, Influence of particle size of zero-valent iron and dissolved silica on the reactivity of activated persulfate for degradation of acid orange 7, Chem. Eng. J., 237 (2014) 487–496.
[41] R.A. Larson, E.J. Weber, Reaction Mechanisms in Environmental Organic Chemistry, CRC Press, Boca Raton, Florida, 1994.
[42] J. Guo, D. Jiang, Y. Wu, P. Zhou, Y. Lan, Degradation of methyl orange by Zn(0) assisted with silica gel, J. Hazard. Mater., 194 (2011) 290–296.
[43] L.P. Yang, W.Y. Hu, H.M. Huang, B. Yan, Degradation of high concentration phenol by ozonation in combination with ultrasonic irradiation, Desal. Wat. Treat., 21 (2010) 87–95.
[44] R. Homlok, E. Takács, L. Wojnárovits, Degradation of organic molecules in advanced oxidation processes: relation between chemical structure and degradability, Chemosphere, 91 (2013) 383–389.
[45] M. Zhang, X. Chen, H. Zhou, M. Murugananthan, Y. Zhang, Degradation of p-nitrophenol by heat and metal ions co-activated persulfate, Chem. Eng. J., 264 (2015) 39–47.
[46] H. Suzuki, S. Araki, H. Yamamoto, Evaluation of advanced oxidation process (AOP) using O_3, UV, and TiO_2 for the degradation of phenol in water, J. Water Process Eng., 7 (2015) 54–60.
[47] C.S. Liu, K. Shih, C.X. Sun, F. Wang, Oxidative degradation of propachlor by ferrous and copper ion activated persulfate, Sci. Total Environ., 416 (2012) 507–512.
[48] X. Wang, L. Wang, J. Li, J. Qiu, C. Cai, H. Zhang, Degradation of Acid Orange 7 by persulfate activated with zero valent iron in the presence of ultrasonic irradiation, Sep. Purif. Technol., 122 (2014) 41–46.
[49] X.-R. Xu, Z.-Y. Zhao, X.-Y. Li, J.-D. Gu, Chemical oxidative degradation of methyl tert-butyl ether in aqueous solution by Fenton's reagent, Chemosphere, 55 (2004) 73–79.
[50] Y.-F. Huang, Y.-H. Huang, Identification of produced powerful radicals involved in the mineralization of bisphenol A using a novel UV-$Na_2S_2O_8$/H_2O_2-Fe(II,III) two-stage oxidation process, J. Hazard. Mater., 162 (2009) 1211–1216.
[51] J. Zhao, Y. Zhang, X. Quan, S. Chen, Enhanced oxidation of 4-chlorophenol using sulfate radicals generated from zero-valent iron and peroxydisulfate at ambient temperature, Sep. Purif. Technol., 71 (2010) 302–307.
[52] J. Yan, M. Lei, L. Zhu, M.N. Anjum, J. Zou, H. Tang, Degradation of sulfamonomethoxine with Fe_3O_4 magnetic nanoparticles as heterogeneous activator of persulfate, J. Hazard. Mater., 186 (2011) 1398–1404.
[53] G.V. Buxton, C.L. Greenstock, W.P. Helman, A.B. Ross, Critical review of rate constants for reactions of hydrated electrons, hydrogen atoms and hydroxyl radicals ($OH^{\bullet}/O^{\bullet-}$) in aqueous solution, J. Phys. Chem. Ref. Data, 17 (1988) 513–886.
[54] L. Zhu, H.-z. Lin, J.-q. Qi, X.-y. Xu, H.-y. Qi, Effect of H_2 on reductive transformation of p-ClNB in a combined ZVI–anaerobic sludge system, Water Res., 46 (2012) 6291–6299.
[55] S. Vinitnantharat, W. Chartthe, A. Pinisakul, Toxicity of reactive red 141 and basic red 14 to algae and waterfleas, Water Sci. Technol., 58 (2008) 1193–1198.
[56] R.H. Waldemer, P.G. Tratnyek, R.L. Johnson, J.T. Nurmi, Oxidation of chlorinated ethenes by heat-activated persulfate: kinetics and products, Environ. Sci. Technol., 41 (2007) 1010–1015.

[57] S.-H. Chang, K.-S. Wang, S.-J. Chao, T.-H. Peng, L.-C. Huang, Degradation of azo and anthraquinone dyes by a low-cost Fe^0/air process, J. Hazard. Mater., 166 (2009) 1127–1133.
[58] Y. Verma, Toxicity assessment of dye containing industrial effluents by acute toxicity test using *Daphnia magna*, Toxicol. Ind. Health, 27 (2010) 41–49.
[59] H.W. Nugteren, M. Janssen-Jurkovícová, B. Scarlett, Removal of heavy metals from fly ash and the impact on its quality, J. Chem. Technol. Biotechnol., 77 (2002) 389–395.
[60] B. Heibati, S. Rodriguez-Couto, A. Amrane, M. Rafatullah, A. Hawari, M.A. Al-Ghouti, Uptake of Reactive Black 5 by pumice and walnut activated carbon: chemistry and adsorption mechanisms, J. Ind. Eng. Chem., 20 (2014) 2939–2947.
[61] B.H. Hameed, A.A. Rahman, Removal of phenol from aqueous solutions by adsorption onto activated carbon prepared from biomass material, J. Hazard. Mater., 160 (2009) 576–581.